Transverse-electric and transverse-magnetic beam modes beyond the paraxial approximation

C. J. R. Sheppard

Department of Physical Optics, School of Physics and The Australian Key Centre for Microscopy and Microanalysis, University of Sydney, Sydney, New South Wales 2006, Australia

S. Saghafi*

Department of Physical Optics, School of Physics, University of Sydney, Sydney, New South Wales 2006, Australia

Received June 18, 1999

Transverse-electric and transverse-magnetic beam modes are considered based on a theory in which complex dipole sources and sinks are oriented along the beam axis; the theory is similar to one that was previously presented for transverse dipoles. The field in the region of the waist is explored. Modes with such polarization have been reported from a wide range of laser types.

OCIS codes: 030.4070, 260.5430, 190.4420.

Modes with TM or TE polarization have been observed from a wide range of different lasers, including solid-state,[1] dye,[2] gas,[3,4] and semiconductor[5] lasers. For paraxial beams these modes have a dark center. Kognelnik and Li[6] showed that in the paraxial approximation such beams can be generated from plane-polarized Laguerre–Gaussian components. Davis and Patsakos[7] generated paraxial TM modes by assuming a magnetic vector potential that was oriented along the axis whose magnitude varied as a Gaussian and also generated TE modes by use of the principle of duality. Later, they presented a model based on the assumption of Whittaker potentials oriented along the axis.[8] Recently, an alternative form of paraxial TE or TM modes based on Bessel–Gaussian beams[9,10] was proposed.[11–16] These beams also exhibit a dark center. A different theory that includes beams with high angles of divergence is based on the complex source-point model, in which a source is assumed to be displaced an imaginary distance along the axis.[17] Cullen and Ku generalized this model to the electromagnetic case by assuming electric or magnetic dipoles oriented in a transverse direction.[18] The complex source-point method results in beams that are rigorous solutions of Maxwell's equations, but a drawback is that there are nonphysical singularities. These singularities can, however, be avoided by assumption of combinations of a source and a sink,[19,20] resulting in beams that are rigorous solutions of Maxwell's equations for all space and that reduce to Gaussian beams in the paraxial limit. The complex source-point method can also be applied to dipoles that are oriented along the axis, thus generating TE and TM beams that are rigorous solutions of Maxwell's equations for all space.

We consider beams based on complex sink–source combinations of either electric or magnetic dipoles oriented along the z axis. Analogous results for transverse dipoles have been derived elsewhere.[19,20] By use of the same approach for the field of a dipole, for the case of an axial electric-dipole combination, the electric field is

$$\mathbf{E} = [f(kR) - g(kR)]\frac{(z - iz_0)(x\mathbf{i} + y\mathbf{j})}{R^2} + \left[f(kR)\frac{(z - iz_0)^2}{R^2} + g(kR)\frac{(x^2 + y^2)}{R^2}\right]\mathbf{k}, \quad (1)$$

where

$$f(kR) = j_0(kR) + j_2(kR) = -3\left[\frac{\cos kR}{(kR)^3} - \frac{\sin kR}{(kR)^3}\right],$$

$$g(kR) = j_0(kR) - \frac{1}{2}j_2(kR) = \frac{3}{2}\left[\frac{\sin kR}{kR} + \frac{\cos kR}{(kR)^2} - \frac{\sin kR}{(kR)^3}\right], \quad (2)$$

where $k = 2\pi/\lambda$, j_n is a spherical Bessel function of the order n, and

$$R = [x^2 + y^2 + (z - iz_0)^2]^{1/2}. \quad (3)$$

The variation in time-averaged electric-energy density along the axes is shown in Fig. 1. The distribution is axially symmetric. For large values of kz_0 the beam reduces to the paraxial form, and the intensity on the axis becomes small compared with the maximum value, giving a dark center. However, for kz_0 less than ~ 10 the maximum intensity is reached on the axis. This is caused by the longitudinal component of the field. For small values of kz_0 there are oscillations in intensity in the waist.

On the axis the electric field is given by

$$\mathbf{E} = f(kR)\mathbf{k}, \quad (4)$$

0146-9592/99/221543-03$15.00/0

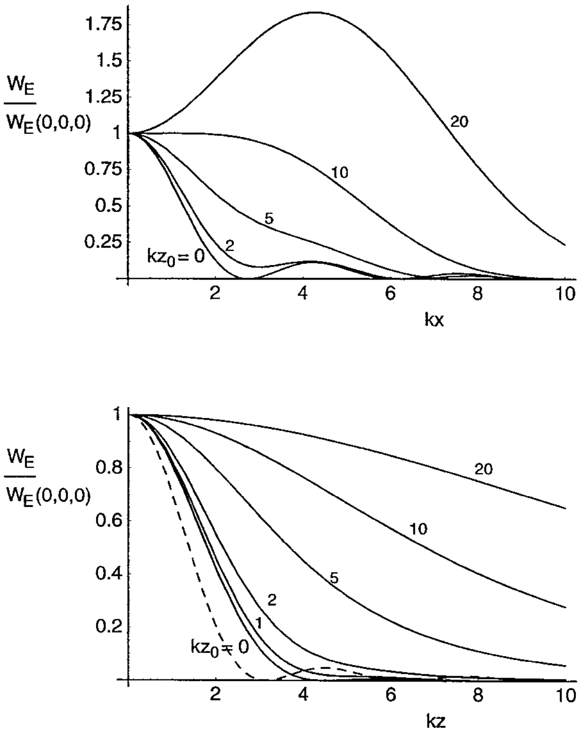

Fig. 1. Variation in time-averaged electric-energy density along the axes for an electric-dipole sink–source combination oriented along the z axis (TM_{01} mode). For large values of kz_0 the beam has a dark center.

so that it is directed along the axis. The phase variation along the axis is shown in Fig. 2. The phase exhibits a Gouy phase anomaly, but unlike in the linearly polarized cases[20,21] the phase changes from $-\pi$ to $+\pi$ when the observation point goes through the focus.

Figure 3 shows contours of constant time-averaged electric-energy density in an azimuthal plane for two different values of $kz_0 = 2$; the maximum intensity is reached at the focus, whereas for $kz_0 = 20$ there is a saddle point at the focus.

The magnetic field, given by[20]

$$\mathbf{H} = \sqrt{\frac{\varepsilon_0}{\mu_0}}\, f(kR)\left(\frac{y}{R}\,\mathbf{i} - \frac{x}{R}\,\mathbf{j}\right), \qquad (5)$$

where ϵ_0 and μ_0 are the permittivity and the permeability of free space, respectively, is purely transverse, so we call this field the TM_{01} beam. The lines of the magnetic field are circles around the axis. The electric-field lines are closed curves in azimuthal planes. For large values of kz_0 the beams tend to resemble those described previously.[7,8]

For the alternative case of magnetic-dipole source–sink combinations, the electric field is[20]

$$\mathbf{E} = -\frac{i}{2} f(kR)\,(ky\mathbf{i} - kx\mathbf{j}), \qquad (6)$$

which is purely transverse. We call this the TE_{01} beam. The electric-field lines are circles around the axis. The time-averaged electric-energy density is axially symmetric, and its variation in the waist is shown in Fig. 4. This figure was plotted directly from Eq. (6), as the intensity cannot be normalized because it is zero on the axis. The behavior of the electric-energy density is not strongly dependent on the value of kz_0, except that the relative strength of the outer rings decreases as kz_0 increases. Figure 5 shows contours of constant time-averaged electric-energy density

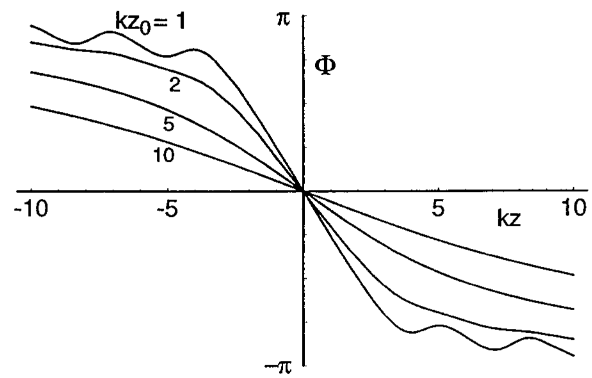

Fig. 2. Phase variation along the axis for an electric-dipole sink–source combination oriented along the z axis (TM_{01} mode).

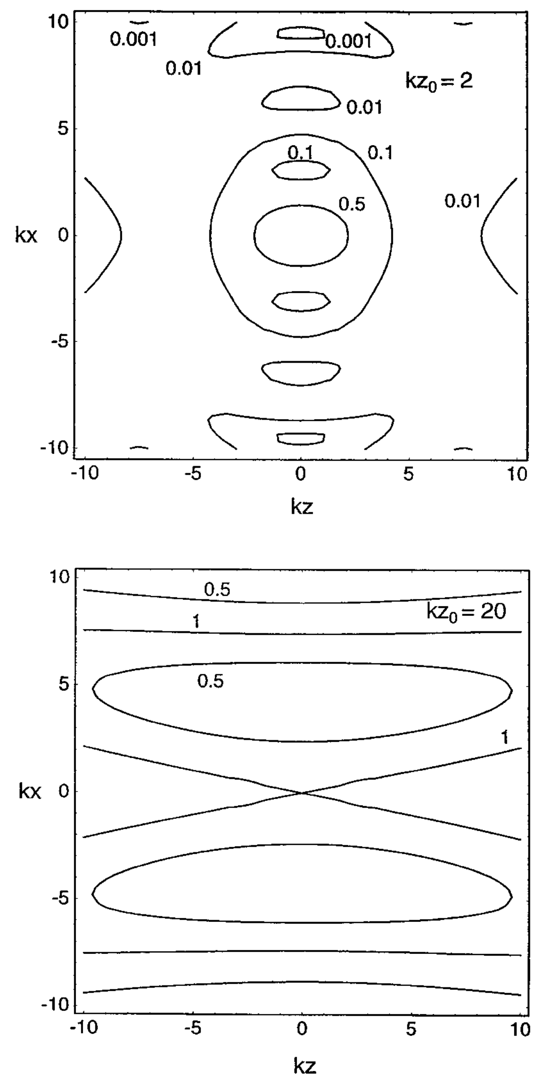

Fig. 3. Contours of constant time-averaged electric-energy density in an azimuthal plane, for an electric-dipole sink–source combination oriented along the z axis, for two different values of kz_0 (TM_{01} mode).

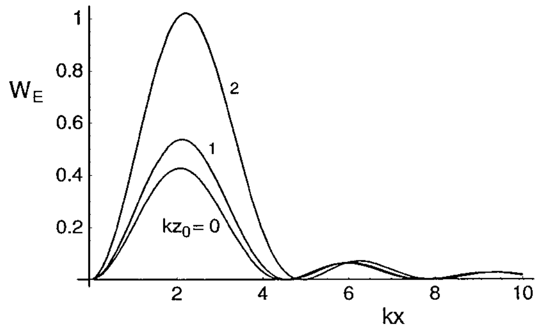

Fig. 4. Variation in the time-averaged electric-energy density (in arbitrary units) in the waist for a magnetic-dipole sink–source combination oriented along the z axis (TE_{01} mode).

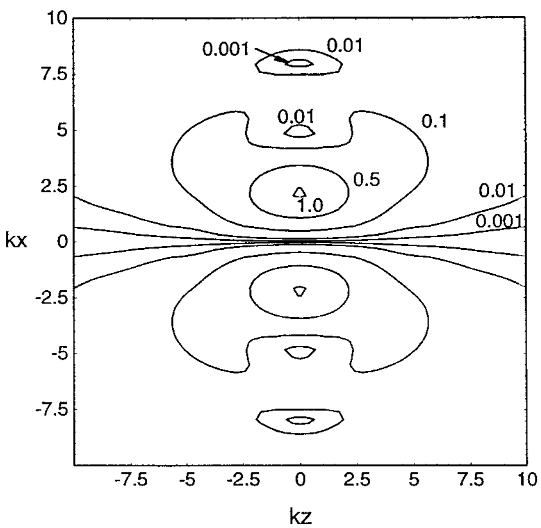

Fig. 5. Contours of constant intensity in an azimuthal plane for magnetic-dipole sink–source combination oriented along the z axis, for $kz_0 = 2$ (TE_{01} mode).

in an azimuthal plane when $kz_0 = 2$. There is a toroidal region of high intensity in the waist region.

TE_{01} and TM_{01} beams can be generated by axially directed electric- and magnetic-dipole source–sink combinations at a complex displacement. These beams are rigorous solutions of Maxwell's equations for all space. Higher-order TE and TM modes can be generated in a similar way to that for linearly polarized beams, by use of multipole fields.[21,22]

The authors acknowledge support from the Australian Research Council and the Science Foundation for Physics within the University of Sydney.
C. J. R. Sheppard's e-mail address is colin@physics.usyd.edu.au.

*Present address: Department of Mathematics, Physics, Macquarie University, New South Wales 2106, Australia.

References

1. D. Pohl, Appl. Phys. Lett. **20,** 266 (1972).
2. J. J. Wynne, IEEE J. Quantum Electron. **QE-10,** 125 (1974).
3. Y. Mushiake, K. Matsumura, and N. Nakajima, Proc. IEEE **60,** 1107 (1972).
4. M. E. Marhic and E. Garmire, Appl. Phys. Lett. **38,** 743 (1981).
5. T. Erdogan, O. King, G. W. Wicks, D. G. Hall, K. Anderson, and M. J. Rooks, Appl. Phys. Lett. **60,** 1921 (1992).
6. H. Kogelnik and T. Li, Proc. IEEE **54,** 1312 (1966).
7. L. W. Davis and G. Patsakos, Opt. Lett. **6,** 22 (1981).
8. L. W. Davis and G. Patsakos, Phys. Rev. A **26,** 3702 (1982).
9. C. J. R. Sheppard and T. Wilson, IEE J. Microwaves Opt. Acoust. **2,** 105 (1978).
10. F. Gori, G. Guatteri, and C. Padovani, Opt. Commun. **64,** 491 (1987).
11. R. H. Jorden and D. G. Hall, Opt. Lett. **19,** 427 (1994).
12. D. G. Hall, Opt. Lett. **21,** 9 (1996).
13. P. L. Greene and D. G. Hall, J. Opt. Soc. Am. A **13,** 962 (1996).
14. A. A. Tovar and G. H. Clark, J. Opt. Soc. Am. A **14,** 3333 (1997).
15. S. R. Seshadri, J. Opt. Soc. Am. A **15,** 2712 (1998).
16. P. L. Greene and D. G. Hall, Opt. Express **4,** 411 (1999); http://epubs.osa.org/opticsexpress.
17. G. A. Deschamps, Electron. Lett. **7,** 684 (1971).
18. A. L. Cullen and P. K. Yu, Proc. R. Soc. London Ser. A **366,** 155 (1979).
19. C. J. R. Sheppard and S. Saghafi, Phys. Rev. A **57,** 2971 (1998).
20. C. J. R. Sheppard and S. Saghafi, J. Opt. Soc. Am. A **16,** 1381 (1999).
21. C. J. R. Sheppard and S. Saghafi, "Electric and magnetic dipole beam modes beyond the paraxial approximation," Optik (to be published).
22. M. Couture and P.-A. Belanger, Phys. Rev. A **24,** 355 (1981).